molecules

MDPI

Communication

Hydroxide-Mediated S_NAr Rearrangement for Synthesis of Novel Depside Derivatives Containing Diaryl Ether Skeleton as Antitumor Agents

Xiang Yu [1,2,†], Yinkai Xi [1,†], Yi Sui [1], Yang Liu [3], Guifen Chen [1], Minjie Zhang [1], Yan Zhang [1], Guoyong Luo [1], Yi Long [1] and Wude Yang [1,*]

1 College of Pharmacy, Guizhou University of Traditional Chinese Medicine, Guiyang 550025, China
2 Guizhou Joint Laboratory for International Cooperation in Ethnic Medicine, Guizhou University of Traditional Chinese Medicine, Guiyang 550025, China
3 School of Basic Medicine, Guizhou University of Traditional Chinese Medicine, Guiyang 550025, China
* Correspondence: ywd_680708@sina.com
† These authors contribute equally to this work.

Abstract: A simple and efficient hydroxide-mediated S_NAr rearrangement was reported to synthesize new depside derivatives containing the diaryl ether skeleton from the natural product barbatic acid. The prepared compounds were determined using ^1H NMR, ^{13}C NMR, HRMS, and X-ray crystallographic analysis and were also screened in vitro for cytotoxicity against three cancer cell lines and one normal cell line. The evaluation results showed that compound **3b** possessed the best antiproliferative activity against liver cancer HepG2 cell line and low toxicity, which made it worth further study.

Keywords: barbatic acid; diaryl ethers; S_NAr rearrangement; antitumor activity

Citation: Yu, X.; Xi, Y.; Sui, Y.; Liu, Y.; Chen, G.; Zhang, M.; Zhang, Y.; Luo, G.; Long, Y.; Yang, W. Hydroxide-Mediated S_NAr Rearrangement for Synthesis of Novel Depside Derivatives Containing Diaryl Ether Skeleton as Antitumor Agents. *Molecules* **2023**, *28*, 4303. https://doi.org/10.3390/molecules28114303

Academic Editor: Carlotta Granchi

Received: 13 April 2023
Revised: 13 May 2023
Accepted: 14 May 2023
Published: 24 May 2023

1. Introduction

Depsides are dimers formed by ester bonds between two aromatic rings, which are the main secondary metabolites of lichens [1]. Previous research reported that depsides had good biological properties, such as antitumor, antioxidant, and antibacterial activities [2–4]. Barbatic acid (**1**, Figure 1) is one kind of depside that was widely discovered from the lichen [5] and was determined to have a variety of biological activities, including anticancer, schistosomicidal, diuretic, and the potential to inhibit the growth of plants and algal [6–9]. However, to the best of our knowledge, little attention has been paid to the further structural modification of barbatic acid for developing potential antitumor agents.

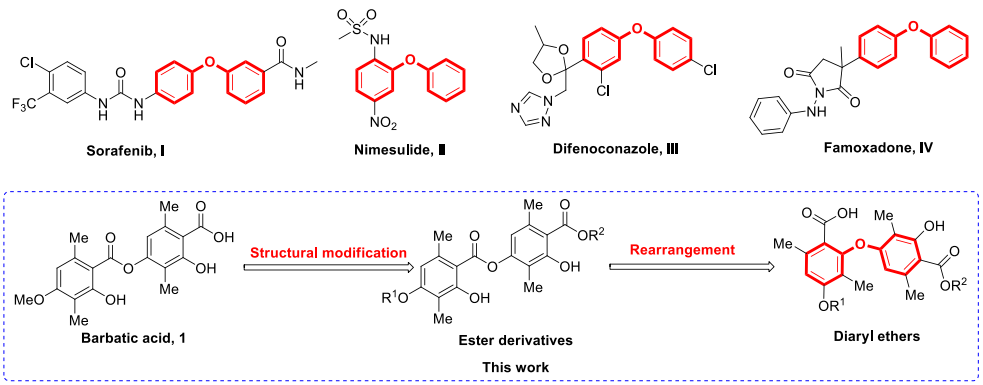

Figure 1. Design of novel diaryl ethers as antitumor agents.

Diaryl ethers are an important class of organic compounds with two aromatic rings and a flexible oxygen bridge, which are widely used in various fields such as medicine

and pesticides [10]. For instance, Sorafenib (**I**, Figure 1) is a highly effective small molecule inhibitor with anticancer properties, which is used to treat advanced renal cancer [11]. Nimesulide (**II**, Figure 1), a nonsteroidal anti-inflammatory drug, has been popularized for several decades [12]. Difenoconazole (**III**, Figure 1) and famoxadone (**IV**, Figure 1) have been utilized as fungicides to protect a wide range of plants, such as rice, cotton, and cereals, from diseases [13,14]. Usually, diaryl ethers are mainly achieved through the coupling of phenols and aryl halides under the action of catalysts to form C–O bonds. These methods have certain deficiencies, such as high temperatures, expensive catalysts, or toxic solvents [15–19].

Herein, we reported an interesting means of converting some barbatic acid esters to novel diaryl ethers through a hydroxide-mediated S_NAr rearrangement reaction. The synthesized compounds were also tested for antitumor activity, and some compounds demonstrated good effects.

2. Results and Discussion

As illustrated in Figure 2, firstly, 3-hydroxy-4-(isopropoxycarbonyl)-2,5-dimethylphenyl 2-hydroxy-4-methoxy-3,6-dimethylbenzoate (**2a**) was prepared by our previously reported method [20]. Subsequently, **2a** reacted with potassium hydroxide in the mixed solvent (DMSO/water = 10/1, v/v) at room temperature. To our delight, the reaction did not undergo hydrolysis to produce corresponding benzoic acid and phenol as we expected but instead underwent a rearrangement reaction to produce diaryl ethers with a yield of 81% (**3a**). This was proven by comparison with the partial ^{1}H NMR spectra of compounds **2a** and **3a** (Figure 3). Compared to compound **2a**, compound **3a** had only one phenolic hydroxyl group, and the chemical shift of aromatic signals was shifted from 6.37 ppm to 5.77 ppm due to the steric effects. There was no significant change in the other chemical shifts. Moreover, the X-ray crystal structure (Figure 4) of compound **3a** further demonstrated this conclusion.

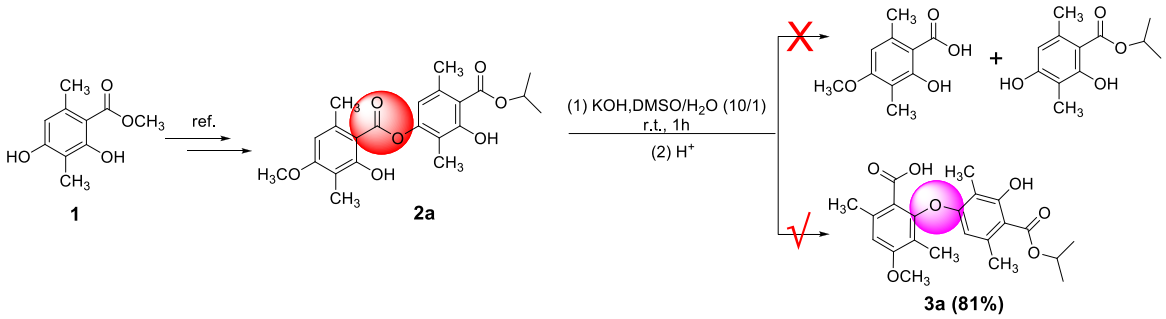

Figure 2. An unanticipated S_NAr reaction leading to **3a**.

In order to test the reliability of the method, compounds **3b–j** continued to be synthesized with a 70–95% yield under the same reaction conditions, as shown in Figure 5. The structures of all target compounds were characterized using ^{1}H NMR, ^{13}C NMR, and HRMS. The stereochemistry of **3d** was further confirmed by X-ray crystallographic analysis (Figure 6).

In addition, a probable reaction mechanism for this rearrangement was proposed and is illustrated in Figure 7. The sequence began with a simple acid-base reaction wherein hydroxide deprotonated the hydroxyl group, as shown in pink in structure **2**. The resulting phenoxide then participated in an intramolecular S_NAr cyclization onto the second ring, as illustrated by the conversion of structure **4** to the spirocyclic intermediate **5**. The re-establishment of aromaticity was accompanied by the formation of the carboxylate anion shown in structure **6**, and then acidification delivered the target structures **3**.

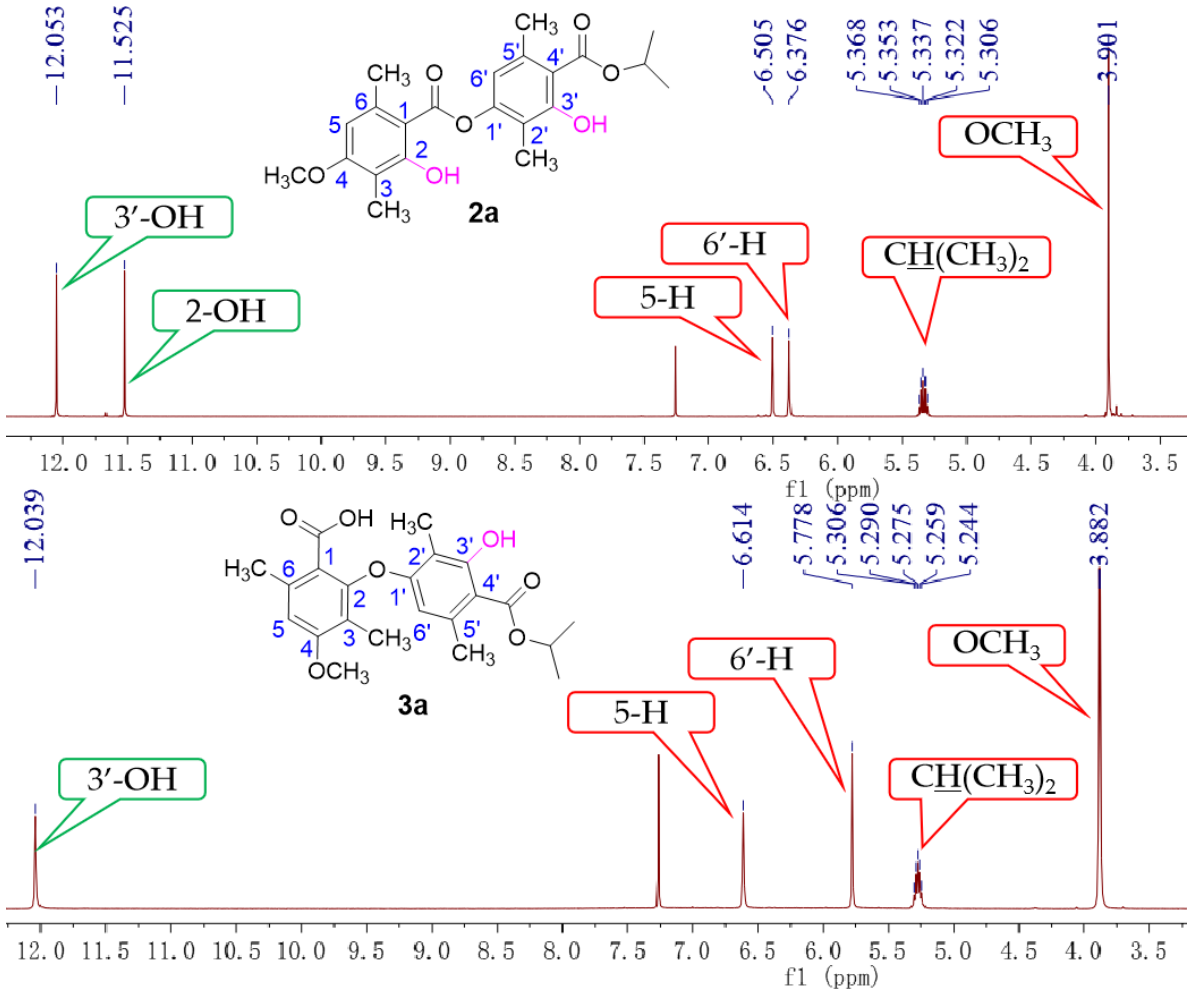

Figure 3. The ^{1}H NMR spectra of **2a** and **3a**.

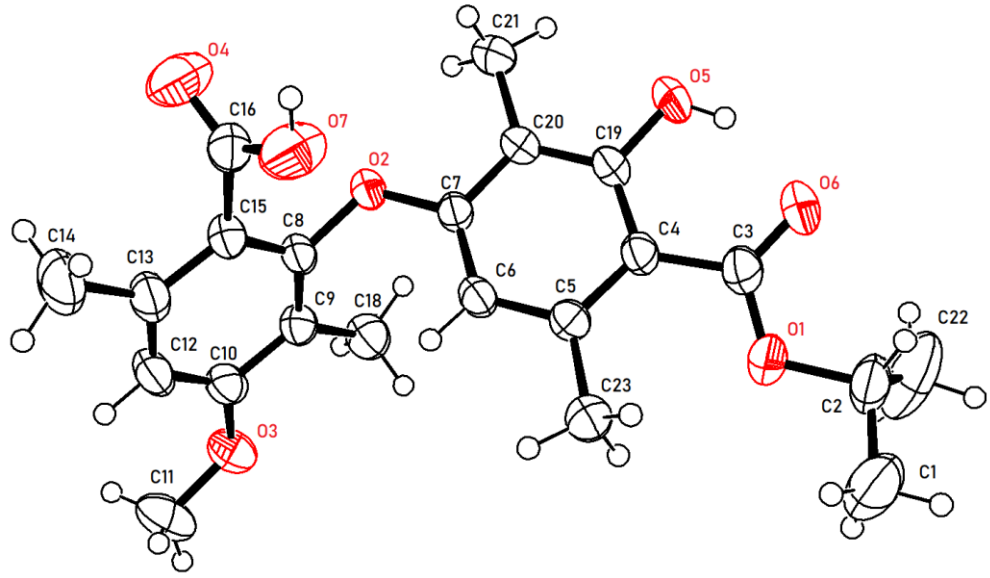

Figure 4. X-ray crystallographic structures of **3a**.

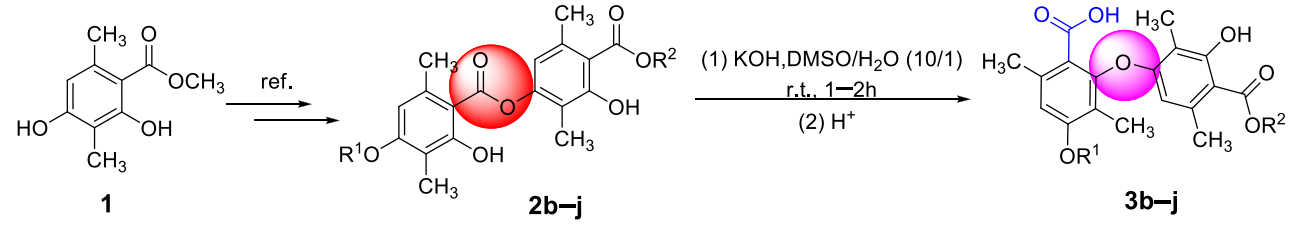

3b: R^1= CH_3, R^2= Bn (73%)
3c: R^1= CH_2CH_3, R^2= Bn (87%)
3d: R^1= $CH_2CH_2CH_3$, R^2= CH_3 (77%)
3e: R^1= $CH_2CH_2CH_3$, R^2= $CH(CH_3)_2$ (95%)
3f: R^1= $CH_2CH_2CH_3$, R^2= Bn (72%)
3g: R^1= $CH(CH_3)_2$, R^2= CH_3 (92%)
3h: R^1= $CH(CH_3)_2$, R^2= Bn (88%)
3i: R^1= Bn, R^2= CH_3 (74%)
3j: R^1= Bn, R^2= CH_2CH_3 (70%)

Figure 5. The synthetic route to compound **3b**–**j**.

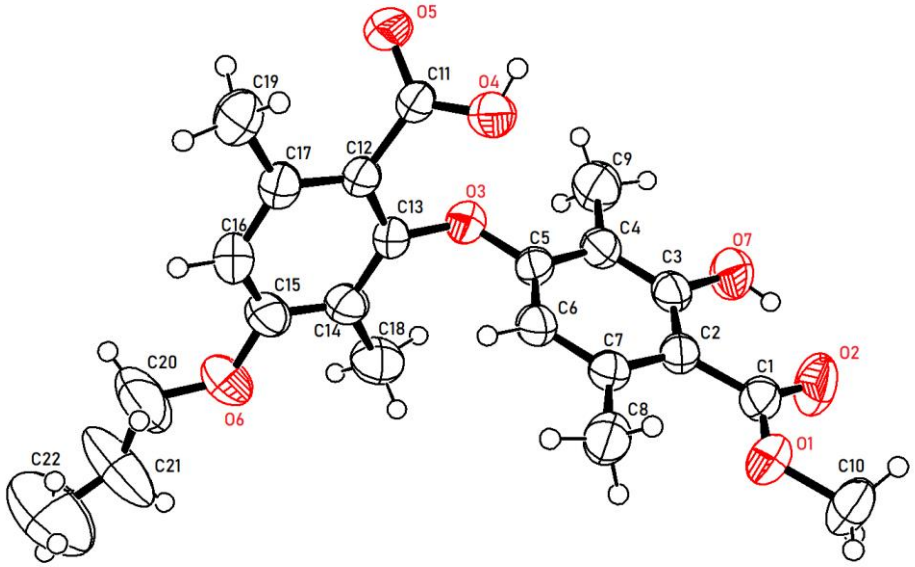

Figure 6. X-ray crystallographic structures of **3d**.

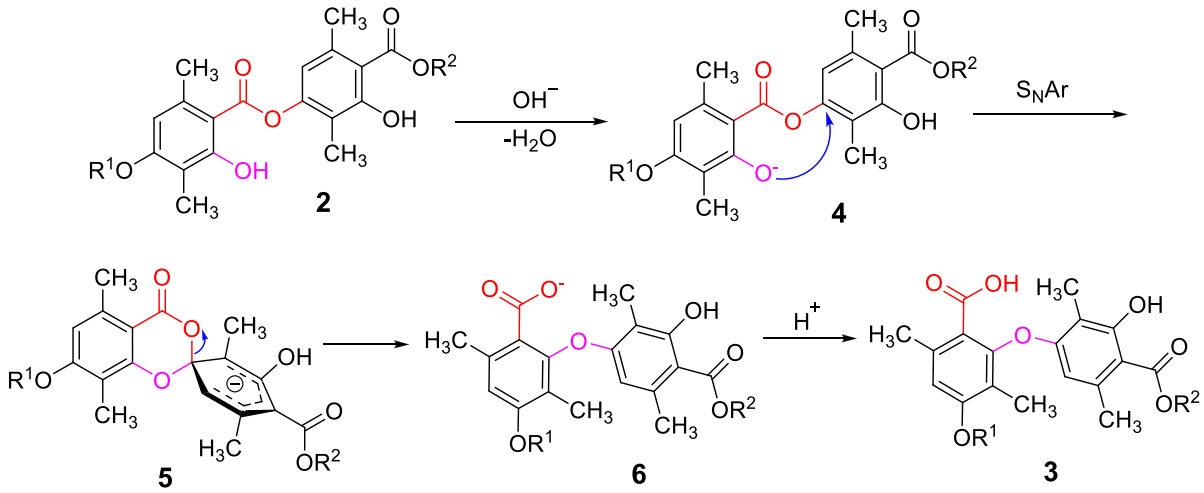

Figure 7. Possible mechanism for synthesis of compounds **3a**–**j**.

Compounds **3a**–**j** were screened for their antitumor activities against three human cancer cell lines (lung cancer A549 cells, liver cancer HepG2 cells, and prostatic cancer 22RV1 cells) in vitro by the standard MTT method, and the IC_{50} values are presented in Table 1. The experimental results showed that compounds **3a**, **3c**, **3e**, and **3f** exhibited moderate cytotoxic activities against A549 cells with IC_{50} values of 2.61, 1.43, and 2.21 mmol/L,

respectively. Compounds **3a–d**, **i–j** induced high cytotoxic activity against HepG2 cells, which exhibited excellent activities with IC_{50} values of 0.41–1.56 mmol/L. Compound **3d** afforded the best antiproliferation activities toward 22RV1 cells, with an IC_{50} value of 0.78 mmol/L. The results demonstrated that diaryl ethers synthesized in this study possessed potential antitumor activities.

Table 1. IC_{50} values (mmol/L) of compounds **3a–j** against three human cancer cell lines.

Compound	A549	HepG2	22RV1
3a	2.61	0.48	32.84
3b	/ [a]	0.82	/
3c	21.52	0.56	/
3d	/	1.26	0.78
3e	1.43	/	/
3f	2.21	/	6.16
3g	14.83	/	/
3h	26.94	/	3.24
3i	/	0.41	/
3j	/	1.56	/

[a] No inhibition action.

Selective killing of cancer cells without affecting normal cell growth is an important feature that must be considered in cancer chemotherapy. Therefore, the target compounds **3a–j** were estimated for cytotoxicity toward normal madin-daby canine kidney cells (MDCK) and as shown in Figure 8. Compared to the blank control, most compounds could influence the growth of normal MDCK cells with cell survival rates below 90%, except for compound **3b** (97.47%), suggesting that **3b** had almost no toxicity to normal cells and could selectively inhibit the growth of liver cancer HepG2 cells.

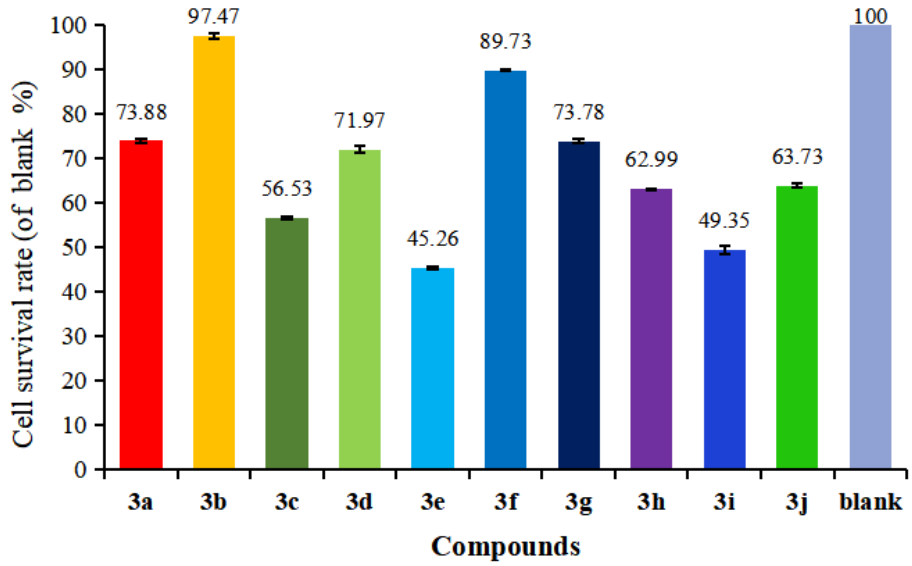

Figure 8. The cytotoxicity of compounds **3a–j** on normal MDCK Cells at 100 μmol/L.

3. Materials and Methods

3.1. Chemistry

All reagents and solvents were of reagent grade or were purified according to standard methods before use. Analytical thin-layer chromatography (TLC) was performed with silica gel plates using silica gel 60 GF_{254} (Qingdao Haiyang Chemical Co., Ltd., Qingdao, China). Melting points were determined on an XT-4 digital melting point apparatus (Beijing Tech Instrument Co., Ltd., Beijing, China) and were uncorrected. Proton nuclear magnetic resonance spectra (^{1}H NMR) were recorded on a Bruker Avance DMX 400 MHz instrument

(Bruker, Bremerhaven, Germany) in $CDCl_3$ or DMSO-d_6 using TMS (tetramethylsilane) as the internal standard. High-resolution mass spectrometry (HRMS) was carried out with a Xevo G2-SQTOF instrument (Waters, Milford, MA, USA).

3.1.1. Synthesis of Intermediates **2a**–**j**

Compounds **2a**–**j** were prepared, as described in our previous publication [20], and their spectra data are shown below.

Data for *3-hydroxy-4-(isopropoxycarbonyl)-2,5-dimethylphenyl 2-hydroxy-4-methoxy-3,6-dimethylbenzoate* (**2a**): Yield: 48%, white solid, mp 135–138 °C; ^{1}H NMR (400 MHz, $CDCl_3$): δ 12.05 (s, 1H), 11.53 (s, 1H), 6.50 (s, 1H), 6.38 (s, 1H), 5.34 (p, J = 6.3 Hz, 1H), 3.90 (s, 3H), 2.69 (s, 3H), 2.55 (s, 3H), 2.10 (s, 3H), 2.08 (s, 3H), 1.41 (d, J = 6.3 Hz, 6H); ^{13}C NMR (100 MHz, $CDCl_3$): δ 171.3, 170.2, 162.9, 162.8, 162.2, 152.3, 140.7, 139.6, 116.9, 116.2, 111.3, 110.4, 106.4, 104.3, 69.8, 55.5, 25.1, 24.2, 21.9 × 2, 9.3, 7.8; HRMS m/z calcd for $C_{22}H_{26}O_7Na$ ([M + Na]$^+$) 425.1570, found 425.1566.

Data for *Benzyl 2-hydroxy-4-((2-hydroxy-4-methoxy-3,6-dimethylbenzoyl)oxy)-3,6-dimethyl benzoate* (**2b**): Yield: 50%, white solid, mp 113–115 °C; ^{1}H NMR (400 MHz, $CDCl_3$): δ 11.92 (s, 1H), 11.51 (s, 1H), 7.48–7.34 (m, 5H), 6.51 (s, 1H), 6.38 (s, 1H), 5.43 (s, 2H), 3.90 (s, 3H), 2.69 (s, 3H), 2.52 (s, 3H), 2.10 (s, 3H), 2.09 (s, 3H); ^{13}C NMR (100 MHz, $CDCl_3$): δ 172.0, 170.6, 163.5 × 2, 162.7, 153.0, 141.2, 140.3, 135.5, 129.2 × 2, 129.1, 128.9 × 2, 117.5, 116.9, 111.8, 110.4, 106.9, 104.8, 67.9, 56.0, 25.5, 24.8, 9.8, 8.3; HRMS m/z calcd. for $C_{26}H_{26}O_7Na$ ([M + Na]$^+$) 473.1570, found 473.1569.

Data for *benzyl 4-(4-ethoxy-2-hydroxy-3,6-dimethylbenzoyloxy)-2-hydroxy-3,6-dimethylbenzoate* (**2c**): Yield: 36%, white solid, mp 129–131 °C; ^{1}H NMR (400 MHz, $CDCl_3$): δ 11.93 (s, 1H), 11.52 (s, 1H), 7.47–7.33 (m, 5H), 6.51 (s, 1H), 6.36 (s, 1H), 5.43 (s, 2H), 4.12 (q, J = 6.8 Hz, 2H), 2.67 (s, 3H), 2.53 (s, 3H), 2.11 (s, 3H), 2.10 (s, 3H), 1.46 (t, J = 6.8 Hz, 3H); ^{13}C NMR (100 MHz, $CDCl_3$): δ 171.6, 170.2, 163.1, 163.0, 161.8, 152.6, 140.6, 139.8, 135.1, 128.7 × 2, 128.6, 128.5 × 2, 117.0, 116.4, 111.3, 109.8, 107.3, 104.1, 67.5, 63.8, 25.1, 24.4, 14.8, 9.3, 7.9; HRMS m/z calcd for $C_{27}H_{28}O_7Na$ ([M + Na]$^+$) 487.1727, found 487.1729.

Data for *3-hydroxy-4-(methoxycarbonyl)-2,5-dimethylphenyl 2-hydroxy-3,6-dimethyl-4-propoxybenzoate* (**2d**): Yield: 33%, white solid, mp 110–113 °C; ^{1}H NMR (400 MHz, $CDCl_3$): δ 11.91 (s, 1H), 11.50 (s, 1H), 6.51 (s, 1H), 6.34 (s, 1H), 4.00 (t, J = 6.4 Hz, 2H), 3.96 (s, 3H), 2.65 (s, 3H), 2.52 (s, 3H), 2.10 (s, 3H), 2.07 (s, 3H), 1.85 (p, J = 6.9 Hz, 2H), 1.06 (t, J = 7.4 Hz, 3H); ^{13}C NMR (100 MHz, $CDCl_3$): δ 172.3, 170.2, 163.0, 162.8, 161.9, 152.5, 140.6, 139.6, 116.9, 116.4, 111.4, 109.9, 107.3, 104.0, 69.7, 52.2, 25.0, 24.0, 22.6, 10.5, 9.3, 7.8; HRMS m/z calcd for $C_{22}H_{26}O_7Na$ ([M + Na]$^+$) 425.1570, found 425.1564.

Data for *3-hydroxy-4-(isopropoxycarbonyl)-2,5-dimethylphenyl 2-hydroxy-3,6-dimethyl-4-propoxybenzoate* (**2e**): Yield: 37%, white solid, mp 112–115 °C; ^{1}H NMR (400 MHz, $CDCl_3$): δ 12.05 (s, 1H), 11.53 (s, 1H), 6.50 (s, 1H), 6.36 (s, 1H), 5.38-5.29 (m, 1H), 4.01 (t, J = 6.4 Hz, 2H), 2.67 (s, 3H), 2.54 (s, 3H), 2.11 (s, 3H), 2.08 (s, 3H), 1.89–1.80 (m, 2H), 1.42 (s, 3H), 1.41 (d, J = 6.3 Hz, 6H), 1.07 (t, J = 7.2 Hz, 3H); ^{13}C NMR (100 MHz, $CDCl_3$): δ 171.3, 170.3, 163.0, 162.8, 161.9, 152.3, 140.6, 139.6, 116.9, 116.3, 111.4, 110.4, 107.3, 104.1, 69.8, 69.7, 25.0, 24.2, 22.6, 21.9 × 2, 10.5, 9.3, 7.8; HRMS m/z calcd for $C_{24}H_{30}O_7Na$ ([M + Na]$^+$) 453.1883, found 453.1883.

Data for *benzyl 2-hydroxy-4-(2-hydroxy-3,6-dimethyl-4-propoxybenzoyloxy)-3,6-dimethylbenzoate* (**2f**): Yield: 30%, white solid, mp 111–114 °C; ^{1}H NMR (400 MHz, $CDCl_3$): δ 11.92 (s, 1H), 11.51 (s, 1H), 7.51–7.29 (m, 5H), 6.51 (s, 1H), 6.36 (s, 1H), 5.43 (s, 2H), 4.02 (t, J = 6.4 Hz, 2H), 2.67 (s, 3H), 2.52 (s, 3H), 2.11 (s, 3H), 2.09 (s, 3H), 1.86 (q, J = 6.5 Hz, 2H), 1.07 (t, J = 7.4 Hz, 3H); ^{13}C NMR (100 MHz, $CDCl_3$): δ 171.6, 170.2, 163.0, 163.0, 161.9, 152.6, 140.6, 139.7, 135.1, 128.7 × 2, 128.6, 128.4 × 2, 117.0, 116.4, 111.4, 109.9, 107.3, 104.1, 69.7, 67.4, 25.0, 24.3, 22.6, 10.5, 9.3, 7.8; HRMS m/z calcd for $C_{28}H_{30}O_7Na$ ([M + Na]$^+$) 501.1883, found 501.1880.

Data for *3-hydroxy-4-(methoxycarbonyl)-2,5-dimethylphenyl 2-hydroxy-4-isopropoxy-3,6-dimethylbenzoate* (**2g**): Yield: 36%, white solid, mp 60–63 °C; ^{1}H NMR (400 MHz, $CDCl_3$): δ 11.92 (s, 1H), 11.53 (s, 1H), 6.51 (s, 1H), 6.37 (s, 1H), 4.67 (p, J = 6.1 Hz, 1H), 3.97 (s, 3H), 2.66 (s, 3H), 2.53 (s, 3H), 2.09 (s, 6H), 1.38 (d, J = 6.0 Hz, 6H); ^{13}C NMR (100 MHz, $CDCl_3$): δ

172.3, 170.2, 163.4, 162.8, 161.0, 152.6, 140.3, 139.6, 116.9, 116.4, 112.3, 109.9, 108.6, 103.8, 70.3, 52.2, 25.1, 24.0, 22.2 × 2, 9.3, 8.0; HRMS *m*/*z* calcd for $C_{22}H_{26}O_7Na$ ([M + Na]$^+$) 425.1570, found 425.1568.

Data for *benzyl 2-hydroxy-4-(2-hydroxy-4-isopropoxy-3,6-dimethylbenzoyloxy)-3,6-dimethylbenzoate* (**2h**): Yield: 40%, white solid, mp 83–86 °C; ^{1}H NMR (400 MHz, $CDCl_3$): *δ* 11.91 (s, 1H), 11.53 (s, 1H), 7.47–7.33 (m, 5H), 6.50 (s, 1H), 6.36 (s, 1H), 5.42 (s, 2H), 4.66 (p, *J* = 6.1 Hz, 1H), 2.65 (s, 3H), 2.51 (s, 3H), 2.08 (s, 6H), 1.37 (d, *J* = 6.0 Hz, 6H); ^{13}C NMR (100 MHz, $CDCl_3$): *δ* 171.6, 170.2, 163.4, 163.0, 161.0, 152.6, 140.3, 139.7, 135.1, 128.7 × 2, 128.6, 128.4 × 2, 117.0, 116.4, 112.3, 109.8, 108.6, 103.8, 70.3, 67.5, 25.1, 24.3, 22.2 × 2, 9.3, 8.0; HRMS *m*/*z* calcd for $C_{28}H_{30}O_7Na$ ([M + Na]$^+$) 501.1883, found 501.1883.

Data for *3-hydroxy-4-(methoxycarbonyl)-2,5-dimethylphenyl 4-(benzyloxy)-2-hydroxy-3,6-dimethylbenzoate* (**2i**): Yield: 35%, white solid, mp 131–134 °C; ^{1}H NMR (400 MHz, $CDCl_3$): *δ* 11.93 (s, 1H), 11.54 (s, 1H), 7.48–7.33 (m, 5H), 6.52 (s, 1H), 6.45 (s, 1H), 5.18 (s, 2H), 3.98 (s, 3H), 2.67 (s, 3H), 2.54 (s, 3H), 2.18 (s, 3H), 2.09 (s, 3H); ^{13}C NMR (100 MHz, $CDCl_3$): *δ* 172.7, 170.6, 163.6, 163.3, 161.8, 152.9, 141.1, 140.1, 137.1, 129.1 × 2, 128.4, 127.5 × 2, 117.3, 116.8, 112.2, 110.4, 108.1, 105.0, 70.4, 52.7, 25.5, 24.4, 9.7, 8.5; HRMS *m*/*z* calcd for $C_{26}H_{26}O_7Na$ ([M + Na]$^+$) 473.1570, found 473.1569.

Data for *4-(ethoxycarbonyl)-3-hydroxy-2,5-dimethylphenyl 4-(benzyloxy)-2-hydroxy-3,6-dimethylbenzoate* (**2j**): Yield: 40%, white solid, mp 123–126 °C; ^{1}H NMR (400 MHz, $CDCl_3$): *δ* 12.00 (s, 1H), 11.54 (s, 1H), 7.47–7.32 (m, 5H), 6.51 (s, 1H), 6.44 (s, 1H), 5.17 (s, 2H), 4.45 (q, *J* = 7.1 Hz, 2H), 2.67 (s, 3H), 2.55 (s, 3H), 2.17 (s, 3H), 2.08 (s, 3H), 1.43 (t, *J* = 7.1 Hz, 3H); ^{13}C NMR (100 MHz, $CDCl_3$): *δ* 171.8, 170.2, 163.1, 162.8, 161.4, 152.4, 140.6, 139.7, 136.6, 128.6 × 2, 128.0, 127.0 × 2, 116.9, 116.3, 111.8, 110.1, 107.6, 104.5, 69.9, 61.7, 25.1, 24.1, 14.2, 9.3, 8.1; HRMS *m*/*z* calcd for $C_{27}H_{28}O_7Na$ ([M + Na]$^+$) 487.1727, found 487.1721.

3.1.2. Synthesis of Target Compounds **3a**–**j**

To a stirred solution of potassium hydroxide (67.3 mg, 1.2 mmol) in a mixed solvent (20 mL, DMSO/water = 10/1, *v*/*v*) at room temperature, **2a**–**j** (0.6 mmol) was added. The reaction mixture was stirred for 1–2 h. Subsequently, the pH of the reaction mixture was adjusted to 1–2 with 1 mol/L hydrochloric acid, and the crude solid was collected by filtration before it was recrystallized with ethanol to afford **3a**–**j** in 70–95%.

Data for *2-(3-hydroxy-4-(isopropoxycarbonyl)-2,5-dimethylphenoxy)-4-methoxy-3,6-dimethylbenzoic* acid (**3a**): Yield: 81%, white solid, mp 206–208 °C; ^{1}H NMR (400 MHz, $CDCl_3$) *δ* 12.04 (s, 1H), 6.61 (s, 1H), 5.78 (s, 1H), 5.27 (p, *J* = 6.3 Hz, 1H), 3.88 (s, 3H), 2.45 (s, 3H), 2.35 (s, 3H), 2.23 (s, 3H), 1.89 (s, 3H), 1.37 (s, 3H), 1.36 (s, 3H); ^{13}C NMR (100 MHz, $CDCl_3$) *δ* 171.6, 162.6, 159.7, 159.6, 150.9, 139.8, 137.0, 134.6, 117.8, 111.1, 109.4, 108.3, 106.5 × 2, 69.1, 55.7, 24.6, 22.0 × 2, 20.6, 8.9, 8.1; HRMS *m*/*z* calcd for $C_{22}H_{26}O_7Na$ ([M + Na]$^+$) 425.1571, found 425.1569 (Figures S1–S3).

Data for *2-(4-(benzyloxycarbonyl)-3-hydroxy-2,5-dimethylphenoxy)-4-methoxy-3,6-dimethylbenzoic* acid (**3b**): Yield: 73%, white solid, mp 186–188 °C; ^{1}H NMR (400 MHz, $CDCl_3$) *δ* 11.90 (s, 1H), 7.43–7.30 (m, 5H), 6.60 (s, 1H), 5.78 (s, 1H), 5.36 (s, 2H), 3.87 (s, 3H), 2.44 (s, 3H), 2.32 (s, 3H), 2.22 (s, 3H), 1.88 (s, 3H); ^{13}C NMR (100 MHz, $CDCl_3$) *δ* 171.8, 169.9, 162.8, 160.0, 159.6, 150.8, 139.9, 136.9, 135.4, 128.6 × 2, 128.4 × 2, 128.3, 119.6, 117.7, 111.2, 109.4, 108.4, 106.0, 66.9, 55.7, 24.7, 20.6, 8.9, 8.1; HRMS *m*/*z* calcd for $C_{26}H_{26}O_7Na$ ([M + Na]$^+$) 473.1570, found 473.1567 (Figures S4–S6).

Data for *2-(4-(benzyloxycarbonyl)-3-hydroxy-2,5-dimethylphenoxy)-4-ethoxy-3,6-dimethylbenzoic acid* (**3c**): Yield: 87%, white solid, mp 190–192 °C; ^{1}H NMR (400 MHz, $CDCl_3$) *δ* 11.90 (s, 1H), 7.45–7.27 (m, 5H), 6.59 (s, 1H), 5.75 (s, 1H), 5.36 (s, 2H), 4.08 (q, *J* = 6.9 Hz, 2H), 2.43 (s, 3H), 2.32 (s, 3H), 2.21 (s, 3H), 1.88 (s, 3H), 1.45 (t, *J* = 6.9 Hz, 3H). ^{13}C NMR (100 MHz, $CDCl_3$) *δ* 171.8, 170.7, 162.9, 159.9, 159.5, 151.3, 139.9, 137.6, 135.5, 128.6 × 2, 128.4 × 2, 128.3, 118.2, 118.1, 111.3, 110.5, 108.3, 106.1, 66.9, 64.0, 24.7, 20.9, 14.7, 9.0, 8.0; HRMS *m*/*z* calcd for $C_{27}H_{28}O_7Na$ ([M + Na]$^+$) 487.1727, found 487.1729 (Figures S7–S9).

Data for *2-(3-hydroxy-4-(methoxycarbonyl)-2,5-dimethylphenoxy)-3,6-dimethyl-4-propoxybenzoic acid* (**3d**): Yield: 77%, white solid, mp 234–236 °C; ^{1}H NMR (400 MHz, $CDCl_3$) *δ* 11.90 (s,

1H), 6.60 (s, 1H), 5.80 (s, 1H), 3.98 (t, *J* = 6.4 Hz, 2H), 3.90 (s, 3H), 2.44 (s, 3H), 2.34 (s, 3H), 2.23 (s, 3H), 1.90 (s, 3H), 1.84 (p, *J* = 7.1 Hz, 2H), 1.06 (t, *J* = 7.4 Hz, 3H). ^{13}C NMR (100 MHz, $CDCl_3$) δ 172.5, 170.0, 162.6, 159.9, 159.3, 151.0, 139.8, 137.2, 118.9, 118.0, 111.1, 110.4, 108.4, 106.1, 69.9, 51.8, 24.4, 22.6, 20.7, 10.6, 8.9, 8.1; HRMS *m*/*z* calcd for $C_{22}H_{26}O_7Na$ ([M + Na]$^+$) 425.1571, found 425.1566 (Figures S10–S12).

Data for *2-(3-hydroxy-4-(isopropoxycarbonyl)-2,5-dimethylphenoxy)-3,6-dimethyl-4-propoxybenzoic* acid (**3e**): Yield: 95%, white solid, mp 226–228 °C; ^{1}H NMR (400 MHz, $CDCl_3$) δ 12.05 (s, 1H), 6.60 (s, 1H), 5.76 (s, 1H), 5.33–5.22 (m, 1H), 3.99 (t, *J* = 6.6 Hz, 2H), 2.45 (s, 3H), 2.35 (s, 3H), 2.21 (s, 3H), 1.89 (s, 3H), 1.84 (dt, *J* = 13.9, 7.0 Hz, 2H), 1.37 (s, 3H), 1.36 (s, 3H), 1.06 (t, *J* = 7.4 Hz, 3H); ^{13}C NMR (100 MHz, $CDCl_3$) δ 171.6, 170.9, 162.7, 159.6, 159.6, 151.3, 139.8, 137.6, 118.2, 118.1, 111.2, 110.4, 108.2, 106.6, 69.9, 69.1, 24.6, 22.6, 22.0 × 2, 20.9, 10.5, 8.9, 8.0; HRMS *m*/*z* calcd for $C_{24}H_{30}O_7Na$ ([M + Na]$^+$) 453.1883, found 453.1878 (Figures S13–S15).

Data for *2-(4-(benzyloxycarbonyl)-3-hydroxy-2,5-dimethylphenoxy)-3,6-dimethyl-4-propoxybenzoic acid* (**3f**): Yield: 72%, white solid, mp 176–178 °C; ^{1}H NMR (400 MHz, $CDCl_3$) δ 11.90 (s, 1H), 7.43-7.29 (m, 5H), 6.60 (s, 1H), 5.76 (s, 1H), 5.36 (s, 2H), 3.98 (t, *J* = 6.5 Hz, 2H), 2.43 (s, 3H), 2.32 (s, 3H), 2.22 (s, 3H), 1.89 (s, 3H), 1.84 (dt, *J* = 13.9, 7.0 Hz, 2H), 1.06 (t, *J* = 7.4 Hz, 3H); ^{13}C NMR (100 MHz, $CDCl_3$) δ 171.8, 162.8, 160.0, 159.9, 159.6, 151.2, 139.9, 137.6, 135.4, 128.6 × 2, 128.4 × 2, 128.3, 118.1, 111.3, 110.5, 108.3, 106.1, 106.1, 69.9, 66.9, 24.7, 22.6, 20.9, 10.5, 8.9, 8.1; HRMS *m*/*z* calcd for $C_{28}H_{30}O_7Na$ ([M + Na]$^+$) 501.1884, found 501.1878 (Figures S16–S18).

Data for *2-(3-hydroxy-4-(methoxycarbonyl)-2,5-dimethylphenoxy)-4-isopropoxy-3,6-dimethylbenzoic acid* (**3g**): Yield: 92%, white solid, mp 232–234 °C; ^{1}H NMR (400 MHz, $CDCl_3$) δ 11.90 (s, 1H), 6.63 (s, 1H), 5.78 (s, 1H), 4.62 (hept, *J* = 6.0 Hz, 1H), 3.90 (s, 3H), 2.43 (s, 3H), 2.34 (s, 3H), 2.21 (s, 3H), 1.87 (s, 3H), 1.37 (s, 6H); ^{13}C NMR (100 MHz, $CDCl_3$) δ 172.5, 171.1, 162.7, 159.8, 158.6, 151.5, 139.8, 137.3, 119.1, 118.2, 112.1, 111.2, 108.3, 106.2, 70.8, 51.8, 24.4 × 2, 22.1, 20.9, 9.2, 8.0; HRMS *m*/*z* calcd for $C_{22}H_{26}O_7Na$ ([M + Na]$^+$) 425.1571, found 425.1563 (Figures S19–S21).

Data for *2-(4-(benzyloxycarbonyl)-3-hydroxy-2,5-dimethylphenoxy)-4-isopropoxy-3,6-dimethylbenzoic acid* (**3h**): Yield: 88%, white solid, mp 156–158 °C; ^{1}H NMR (400 MHz, $CDCl_3$) δ 11.90 (s, 1H), 7.44–7.29 (m, 5H), 6.62 (s, 1H), 5.76 (s, 1H), 5.36 (s, 2H), 4.61 (hept, *J* = 6.1 Hz, 1H), 2.43 (s, 3H), 2.32 (s, 3H), 2.21 (s, 3H), 1.86 (s, 3H), 1.40-1.33 (m, 6H); ^{13}C NMR (100 MHz, $CDCl_3$) δ 171.8, 170.6, 162.8, 159.9, 158.6, 151.5, 139.9, 137.4, 135.4, 128.6 × 2, 128.4 × 2, 128.3, 119.1, 118.1, 112.2, 111.3, 108.3, 106.1, 70.8, 66.9, 24.7 × 2, 22.1, 20.9, 9.2, 8.0; HRMS *m*/*z* calcd for $C_{28}H_{30}O_7Na$ ([M + Na]$^+$) 501.1883, found 501.1884 (Figures S22–S24).

Data for *4-(benzyloxy)-2-(3-hydroxy-4-(methoxycarbonyl)-2,5-dimethylphenoxy)-3,6-dimethylbenzoic acid* (**3i**): Yield: 74%, white solid, mp 223–225 °C; ^{1}H NMR (400 MHz, $CDCl_3$) δ 11.91 (s, 1H), 7.48–7.31 (m, 5H), 6.70 (s, 1H), 5.80 (s, 1H), 5.13 (s, 2H), 3.90 (s, 3H), 2.44 (s, 3H), 2.34 (s, 3H), 2.23 (s, 3H), 1.95 (s, 3H); ^{13}C NMR (100 MHz, $CDCl_3$) δ 172.5, 169.9, 162.6, 159.9, 158.8, 151.0, 139.9, 137.0, 136.6, 128.6 × 2, 128.0, 127.2 × 2, 119.7, 118.3, 111.1, 110.8, 108.4, 106.2, 70.3, 51.8, 24.4, 20.6, 9.2, 8.1; HRMS *m*/*z* calcd for $C_{26}H_{26}O_7Na$ ([M + Na]$^+$) 473.1571, found 473.1564 (Figures S25–S27).

Data for *4-(benzyloxy)-2-(4-(ethoxycarbonyl)-3-hydroxy-2,5-dimethylphenoxy)-3,6-dimethylbenzoic* acid (**3j**): Yield: 70%, white solid, mp 184-186 °C; ^{1}H NMR (400 MHz, $CDCl_3$) δ 11.99 (s, 1H), 7.50–7.31 (m, 5H), 6.71 (s, 1H), 5.78 (s, 1H), 5.14 (s, 2H), 4.38 (q, *J* = 7.1 Hz, 2H), 2.44 (s, 3H), 2.36 (s, 3H), 2.22 (s, 3H), 1.95 (s, 3H), 1.38 (t, *J* = 7.1 Hz, 3H); ^{13}C NMR (100 MHz, $CDCl_3$) δ 172.1, 170.4, 162.7, 159.7, 159.0, 151.2, 139.9, 137.4, 136.5, 128.6 × 2, 128.1, 127.2 × 2, 119.2, 118.4, 111.2, 110.9, 108.3, 106.4, 70.3, 61.2, 24.5, 20.8, 14.2, 9.2, 8.1; HRMS *m*/*z* calcd for $C_{27}H_{28}O_7Na$ ([M + Na]$^+$) 487.1727, found 487.1725 (Figures S28–S30).

3.2. In Vitro Cytotoxicity Assay

The cytotoxicity of test compounds against three different tumor cell lines (A549 cells, HepG2 cells, and 22RV1 cells) and one normal cell line (madin-daby canine kidney cells, DMCK) were evaluated using an MTT assay in vitro [21]. Logarithmic growth phase cells were seeded in a 96-well plate (10^4 cells/well) and incubated in a cell culture incubator for

24 h. The culture medium was then removed and replaced with a drug-containing medium for the treatment groups (**3a–j**, 100 μmol/L) and normal saline for the control group. Each well was treated with 100 μL of the respective solution and incubated for an additional 24 h. The culture medium was then removed and replaced with a DMEM solution containing 20 μL of MTT (5 mg/mL). After incubating for 4 h, the liquid in each well was removed and replaced with 150 μL of DMSO, which was shaken for 10 min to ensure thorough mixing. The absorbance at 490 nm was measured to determine the optical density (OD) of each well. Cell growth inhibition rate (%) = $(OD_{Blank} - OD_{Experimental})/OD_{Blank} \times 100\%$. Cell survival rate (%) = $OD_{Experimental}/OD_{Blank} \times 100\%$. Subsequently, the inhibition rates versus seven concentrations of **3a–j** against A549 cells, HepG2 cells, and 22RV1 cells were obtained, and then IC_{50} values were calculated according to the Logit method.

4. Conclusions

In summary, we have described an interesting S_NAr rearrangement to convert barbatic acid ester derivatives to novel diaryl ethers. The products were characterized by ^1H NMR, ^{13}C NMR, HRMS, and X-ray crystallographic analysis. In vitro, anticancer activity tests on a panel of three human cancer cell lines and one normal cell line using an MTT assay revealed that the compound **3b** had excellent activity for HepG2 cell lines and low toxicity, which could be used as a valuable lead compound for further study.

Supplementary Materials: The following supporting information can be downloaded at: https://www.mdpi.com/article/10.3390/molecules28114303/s1. Figures S1–S30: ^1H NMR, ^{13}C NMR and HRMS spectrum of the compounds **3a–j**.

Author Contributions: Data curation, X.Y., Y.X., Y.S., G.C., M.Z. and Y.L. (Yang Liu); formal analysis, X.Y. and Y.Z.; resourse: G.L. and Y.L. (Yi Long); methodology, X.Y., Y.X. and Y.S.; project administration, X.Y. and W.Y.; supervision, W.Y.; writing—original draft, X.Y., Y.S. and Y.Z.; writing—review and editing, X.Y. and W.Y. All authors have read and agreed to the published version of the manuscript.

Funding: This work was supported by the National Natural Science Foundation of China (82160773), the Guizhou Provincial Natural Science Foundation [QKHJ-ZK(2022)G503], Science and Technology Planning Project of Guizhou Province [QKHF-ZK(2023)G426] and the Natural Science Foundation of Guizhou Provincial Department of Education (QJH-KY [2021]068).

Institutional Review Board Statement: Not applicable.

Informed Consent Statement: Not applicable.

Data Availability Statement: Data are included within the manuscript or the Supporting Information File.

Conflicts of Interest: The authors declare no conflict of interest.

Sample Availability: Not applicable.

References

1. Ullah, M.; Uddin, Z.; Song, Y.H.; Li, Z.P.; Kim, J.Y.; Ban, Y.J.; Park, K.H. Bacterial neuraminidase inhibition by phenolic compounds from *Usnea longissima*. *S. Afr. J. Bot.* **2019**, *120*, 326–330. [CrossRef]
2. Zhou, R.; Yang, Y.; Park, S.Y.; Nguyen, T.T.; Seo, Y.W.; Lee, K.H.; Lee, J.H.; Kim, K.K.; Hur, J.S.; Kim, H. The lichen secondary metabolite atranorin suppresses lung cancer cell motility and tumorigenesis. *Sci. Rep.* **2017**, *7*, 8136. [CrossRef] [PubMed]
3. Lohézic-Le Dévéhat, F.; Tomasi, S.; Elix, J.A.; Bernard, A.; Rouaud, I.; Uriac, P.; Boustie, J. Stictic acid derivatives from the lichen *Usnea articulata* and their antioxidant activities. *J. Nat. Prod.* **2007**, *70*, 1218–1220. [CrossRef]
4. Honda, N.K.; Pavan, F.R.; Coelho, R.G.; de Andrade Leite, S.R.; Micheletti, A.C.; Lopes, T.I.; Misutsu, M.Y.; Beatriz, A.; Brum, R.L.; Leite, C.Q. Antimycobacterial activity of lichen substances. *Phytomedicine* **2010**, *17*, 328–332. [CrossRef]
5. Martins, M.C.; Silva, M.C.; Silva, H.A.; Silva, L.R.; Albuquerque, M.C.; Aires, A.L.; Falcão, E.P.; Pereira, E.C.; de Melo, A.M.; da Silva, N.H. Barbatic acid offers a new possibility for control of biomphalaria glabrata and schistosomiasis. *Molecules* **2017**, *22*, 568. [CrossRef] [PubMed]
6. Reddy, S.D.; Siva, B.; Kumar, K.; Babu, V.S.P.; Sravanthi, V.; Boustie, J.; Nayak, V.L.; Tiwari, A.K.; Rao, C.H.V.; Sridhar, B.; et al. Comprehensive analysis of secondary metabolites in usnea longissima (lichenized ascomycetes, parmeliaceae) using UPLC-ESI-QTOF-MS/MS and pro-apoptotic activity of barbatic acid. *Molecules* **2019**, *24*, 2270. [CrossRef]

7. Silva, H.A.M.F.; Aires, A.L.; Soares, C.L.R.; Sá, J.L.F.; Martins, M.C.B.; Albuquerque, M.C.P.A.; Silva, T.G.; Brayner, F.A.; Alves, L.C.; Melo, A.M.M.A.; et al. Barbatic acid from *Cladia aggregata* (lichen): Cytotoxicity and in vitro schistosomicidal evaluation and ultrastructural analysis against adult worms of Schistosoma mansoni. *Toxicol. In Vitro* **2020**, *65*, 104771. [CrossRef] [PubMed]
8. Hager, A.; Brunauer, G.; Türk, R.; Stocker-Wörgötter, E. Production and bioactivity of common lichen metabolites as exemplified by *Heterodea muelleri* (Hampe) Nyl. *J. Chem. Ecol.* **2008**, *34*, 113–120. [CrossRef]
9. Takahagi, T.; Ikezawa, N.; Endo, T.; Ifuku, K.; Yamamoto, Y.; Kinoshita, Y.; Takeshita, S.; Sato, F. Inhibition of PSII in atrazine-tolerant tobacco cells by barbatic acid, a lichen-derived depside. *Biosci. Biotechnol. Biochem.* **2006**, *70*, 266–268. [CrossRef] [PubMed]
10. Chen, T.; Xiong, H.; Yang, J.F.; Zhu, X.L.; Qu, R.Y.; Yang, G.F. Diaryl ether: A privileged scaffold for drug and agrochemical discovery. *J. Agric. Food Chem.* **2020**, *68*, 9839–9877. [CrossRef]
11. Abdelgalil, A.A.; Alkahtani, H.M.; Al-Jenoobi, F.I. Sorafenib. *Profiles Drug Subst. Excip. Relat. Methodol.* **2019**, *44*, 239–266.
12. Rainsford, K.D. Members of the Consensus Report Group on Nimesulide. Nimesulide—A multifactorial approach to inflammation and pain: Scientific and clinical consensus. *Curr. Med. Res. Opin.* **2006**, *22*, 1161–1170. [CrossRef] [PubMed]
13. Dong, F.; Li, J.; Chankvetadze, B.; Cheng, Y.; Xu, J.; Liu, X.; Li, Y.; Chen, X.; Bertucci, C.; Tedesco, D.; et al. Chiral triazole fungicide difenoconazole: Absolute stereochemistry, stereoselective bioactivity, aquatic toxicity, and environmental behavior in vegetables and soil. *Environ. Sci. Technol.* **2013**, *47*, 3386–3394. [CrossRef] [PubMed]
14. Feng, X.; Wang, K.; Pan, L.; Xu, T.; Zhang, H.; Fantke, P. Measured and modeled residue dynamics of famoxadone and oxathiapiprolin in tomato fields. *J. Agric. Food Chem.* **2018**, *66*, 8489–8495. [CrossRef]
15. Zhang, G.; Liu, C.; Yi, H.; Meng, Q.; Bian, C.; Chen, H.; Jian, J.X.; Wu, L.Z.; Lei, A. External oxidant-free oxidative cross-coupling: A photoredox cobalt-catalyzed aromatic c-h thiolation for constructing c-s bonds. *J. Am. Chem. Soc.* **2015**, *137*, 9273–9280. [CrossRef] [PubMed]
16. Moreno, D.R.; Giorgi, G.; Salas, C.O.; Tapia, R.A. New short strategy for the synthesis of the dibenz[b,f]oxepin scaffold. *Molecules* **2013**, *18*, 14797–14806. [CrossRef]
17. Zhai, Y.; Chen, X.; Zhou, W.; Fan, M.; Lai, Y.; Ma, D. Copper-catalyzed diaryl ether formation from (hetero)aryl halides at low catalytic loadings. *J. Org. Chem.* **2017**, *82*, 4964–4969. [CrossRef]
18. Ma, D.; Cai, Q. N,N-dimethyl glycine-promoted Ullmann coupling reaction of phenols and aryl halides. *Org. Lett.* **2003**, *5*, 3799–37802. [CrossRef]
19. Chen, G.; Chan, A.S.C.; Kwong, F.Y. Palladium-catalyzed C–O bond formation: Direct synthesis of phenols and aryl/alkyl ethers from activated aryl halides. *Tetrahedron Lett.* **2007**, *48*, 473–476. [CrossRef]
20. Yu, X.; Xi, Y.K.; Luo, G.Y.; Long, Y.; Yang, W.D. Synthesis of barbacic acid. *J. Asian Nat. Prod. Res.* **2022**, *24*, 1150–1156. [CrossRef]
21. Zhong, Y.; Li, H.N.; Zhou, L.; Su, H.S.; Cheng, M.S.; Liu, Y. Synthesis and antitumor activity evaluation of oleanolic acid saponins bearing an acetylated l-arabinose moiety. *Carbohydr. Res.* **2021**, *503*, 108311. [CrossRef] [PubMed]